Time Varying Computerized Ionospheric Tomography

[1]H. Na and [2]E. Sutton

[1]Department of Electrical Engineering, UCLA, Los Angeles, CA 90095-1594
[2]Rockwell International, Cedar Rapids, IA 52498

Abstract

1996

Computerized ionospheric tomography algorithms traditionally ignore the time variations of ionospheric distributions. Movement of ionospheric features thus becomes a source of degradation in the reconstructed images. This paper presents a new algorithm for imaging time varying ionospheric features. Since additional data sources are critical for accurate time varying reconstructions which are not overly dependent upon a priori assumptions and models, this paper also analyzes the potential contributions of GPS, DMSP and ionosonde data for time-varying image reconstruction.

Introduction

Computerized ionospheric tomography (CIT) algorithms model the ionosphere as a static distribution [1-10]. This assumes that any time variations in the ionosphere occur on much slower time scales than the motion of the satellite across the data acquisition system. The ionosphere, however, contains many features for which this assumption is not valid. As a result, motion of the ionosphere is a source of image degradation for static CIT reconstructions. In addition, static CIT algorithms, by definition, do not reconstruct motion of the ionosphere. This paper therefore introduces a new time varying CIT algorithm (TVCIT) which permits examination of time varying ionospheric features. The time variations are taken into account by adding a third dimension of time to the existing two-dimensional model.

In the traditional static CIT model, a set of densely spaced TEC measurements are available. These TEC measurements however are limited in coverage. The reconstruction problem therefore becomes a mixed under and over determined problem. Adding the time variable to the model without additional data only serves to produce a further underdetermined system. The results obtained from reconstructing with only TEC measurements are therefore poor in quality or overly determined by a priori information. One solution is to incorporate additional data sources into the reconstruction process. TEC measurements from global positioning system (GPS) satellites, and electron density measurements from ionosondes located on the Earth and ionosondes located on defense meteorological satellite program (DMSP) satellites are possible additional sources of data. Each source of data fills out a different section of the altitude-latitude-time volume and provides information about a different subspace of the solution space. This paper will present an analysis of the effect of combining various types of data and discuss the amount of information contained in each combination.

Three-Dimensional System Model

The pattern of TEC data from a navy navigation satellite system (NNSS) satellite is shown on Figure 1. The TEC paths form a fan beam originating at the satellite that sweeps across the image plane in about 20 minutes. With only NNSS data, features can be tracked only while they are within the fan beam. The NNSS data can be collected for closely spaced satellite angles so is very dense in the altitude-latitude plane.

The pattern of TEC data from two GPS satellites is shown in Figure 2. The GPS satellites are at a much higher altitude than the NNSS satellite, so the GPS satellite locations are not shown in the figure. The GPS satellites travel much slower than the NNSS satellites, so for static ionospheric tomography more than one sample for each satellite and receiver would be redundant; however, for time varying ionospheric tomography the GPS data helps considerably to fill in the altitude-latitude-time volume. TEC data from both NNSS and GPS satellites is lacking information on the vertical distribution of electron density. Vertical information can be supplied by either a bottom side or top side ionosonde. Ionosonde data is fundamentally different from TEC data. An ionosonde gives the actual value of electron density in a line above a bottom side ionosonde or below a top side ionosonde. The ionosonde data only reaches as far as the peak electron density.

Figure 3 shows the pattern of data from three bottom side ionosondes. Bottom side ionosonde data is very sparse in the altitude-latitude plane but can be collected at closely spaced intervals of time. Thus a static reconstruction from bottom side ionosonde data alone would be of extremely poor quality. The lines where ionosonde data is available are shown the same length in the diagram, but in reality the lines would be different lengths depending on the height of the peak electron density.

Figure 4 shows the pattern of data from a top side ionosonde. If top side ionosonde data is sampled at closely spaced intervals of time, then it can be very dense in the altitude-latitude plane. Thus a static reconstruction using only top side ionosonde data could be of very good quality for the top side. However, top side ionosonde information does not fill the altitude-latitude-time volume as well as data from several bottom side ionosondes.

Basis Functions for the TVCIT Algorithm

Even with additional sources of data, the solution to the time varying problem is not unique. A priori information is used to reduce the number of unknown parameters. The reduction in the number of unknown parameters has two benefits; the size of the computational problem is reduced, and the number of dimensions of the null space is reduced.

Figure 5 shows the shape of one basis function in the altitude-latitude-time volume. The basis functions are pixels in the horizontal and temporal directions and smoothly varying functions of altitude in the vertical direction.

Figure 6 shows the basis functions in the altitude direction. Each basis function like the one shown in Figure 5 varies in intensity according to one of the profiles shown in Figure 6. The vertical basis functions are calculated from a set of model ionosphere profiles allowing the number of basis functions in the vertical direction to be significantly reduced.

Due to the sparsity of data, localized basis functions must be used in the horizontal and temporal directions. Localized basis functions are functions that are nonzero in only a small area of the image; pixels are the simplest example of localized basis functions. Often when nonlocalized basis functions are used, the reconstruction tends to diverge in areas where there is inadequate data. For time varying reconstruction, the data is much more sparse than for static reconstruction, so if the solution tends to diverge when there is insufficient data, then the solution will diverge in large areas of the three dimensional reconstruction space. The time varying algorithm must be capable of extrapolating through areas of the reconstruction where data is incomplete. Therefore pixels are used in the horizontal and temporal directions along with smoothness constraints.

Even with additional sources of data and vertical basis functions based on a priori information, the solution to the time varying problem is not unique. Therefore, smoothness constraints similar to those used by Fehmers for static reconstruction are used to ultimately select a unique solution from the set of all possible solutions [Fehmers94,Fehmers96].

The TVCIT Algorithm

The equation that simulates the TEC values is

$$Ax = b$$

(1)

where b contains the TEC values, x contains the image data, and

A converts from image domain to TEC data domain. Likewise, the equation that simulates the additional measurements is

(2)

$$Cx = d$$

where d contains the additional measurements, x contains the image data, and C converts from image domain to data domain. Both equations (1) and (2) are mixed under and over determined. Even when both equations (1) and (2) are considered together, the solution is not uniquely determined. In addition, TEC data and other data are difficult to combine, because the relative weighting between the two different kinds of data is not well defined; for all data types, it is assumed that the errors due to spatial and temporal quantization are greater than the measurement errors. The problem of relative weighting between TEC and other data can be solved by separating the two sets of data, i.e. satisfying one set of data before the other. Since TEC data covers the reconstruction volume most evenly, the TEC data should be

satisfied first. Therefore, the time varying algorithm satisfies the TEC data first, then the other data, and finally applies smoothness constraints to determine a unique solution.

First, find the set A_s of solutions x that minimizes

$$J_1(x) = \|Ax - b\|^2$$ (3)

This is illustrated in Figure 7. The letter O designates the origin of the coordinate system. The null space of A is the set of solutions to $Ax = 0$ and always contains the origin. The set A_s is the null space of A translated by the minimum norm solution x_{A_s} of (3). Then, find the subset C_s of A_s containing the solutions $x \in A_s$ that minimizes

$$J_2(x) = \|Cx - d\|^2.$$ (4)

Referring to Figure 7, the null space of CV_A is in a translated and rotated coordinate system where x_{A_s} functions as the origin. The solution set C_s of (3) and (4) together is the null space of CV_A translated by the minimum norm solution x_{C_s}.

Finally, determine the unique solution from the set C_s that minimizes

$$J_3(x) = \|Ex\|^2.$$ (5)

The function $|Ex|$ is a measure of how unsmooth the image is. E is of full rank since the only perfectly smooth image is $x=0$. Therefore, this last step defines a unique solution x.

This three step process is implemented using the singular value decomposition (SVD). The information carried forward from the first to the second step and from the second to the third step consists of a minimum norm solution and a matrix containing an orthonormal basis for the null space. At the completion of the third step, the solution set has been reduced to a single point.

Simulations

Six combinations of data sources will be considered in this section:

1. NNSS alone.
2. NNSS and GPS.
3. NNSS and ionosonde.
4. NNSS and DMSP.
5. NNSS, GPS, and ionosonde.
6. NNSS, GPS, and DMSP.

The combination NNSS, DMSP, and ionosonde is omitted from the list, because it is not likely that the expense of several ionosondes could be justified if DMSP data were available. Similarly, the combination of all four data sources is omitted from the list as unrealistic. Each of the six combinations of data sources will be discussed, and simulations will be presented to show which combinations of data sources are feasible for time varying ionospheric tomography.

Data was simulated using the test image of Figure 8. Simulations were run using each of the six combinations of data sources. For each combination of data sources, simulations were run with the ionosphere static, moving north, and moving south. The NNSS data was collected for 13 ground stations located every 5degree from -30 degrees to 30 degrees latitude, 156 satellite positions from -39 degrees to 39 degrees latitude. Two GPS satellites were used, one at -25 degrees latitude and the other at 25 degrees latitude in the imaging plane. Each ground station was assumed to have a GPS receiver in addition to the NNSS receiver. A total of either 7 or 3 ionosondes were used. If 7 ionosondes were used, then they were evenly spaced from -30 degrees to 30 degrees latitude. If 3 ionosondes were used, then they were placed at -20 degrees, 0 degrees, and 15 degrees latitude. 6 scans from each ionosonde were used, evenly spaced in time. The number of samples from each ionosonde scan averages around 14, depending upon the altitude of the peak electron density. The DMSP satellite was assumed to be in the same position as the NNSS satellite. 20 DMSP scans were used, evenly spaced in time, with approximately 68 samples per scan, depending on the altitude of the peak electron density.

Figure 9 shows a time varying reconstruction of a static ionosphere using NNSS, GPS, and ionosonde data. Six time slices were reconstructed at intervals of 273 seconds. Three vertical basis functions were used, and 27 pixels in the horizontal direction were used. Thus there are a total of 486 unknowns. Figure 10 shows a reconstruction of an ionosphere moving north by 5 degrees during data collection. The movement is from 2.5 degrees south of center to 2.5 degrees north of center.

As can be seen from the reconstructions, this combination of data sources provides enough information to reconstruct both the variation in altitude of the peak electron density, and the horizontal movement of the ionosphere. The reconstructions tend to appear noisier as the amount of movement increases due to the uneven coverage of the ionosondes. This is because the resolution directly above an ionosonde is much better than the resolution between ionosondes, so as features move past the ionosonde, the changing resolution causes distortions in the reconstruction.

In order to show the horizontal movement of the ionosphere, a horizontal slice through the electron density at an altitude of 450 kilometers is shown in Figure 11. It is clear from Figure 11b and Figure 11c that the 5 degrees movement of the ionosphere is accurately reconstructed. The dashed line shows the path of the NNSS satellite.

Figure 12 shows a time varying reconstruction of a static ionosphere using only TEC data from a single NNSS satellite. The data are not sufficient to define the vertical structure of the electron density distribution. Figure 13 shows horizontal slices through the reconstruction using only NNSS data. The horizontal slices though the time varying ionosphere reconstruction show that the horizontal movement is not reconstructed.

Figure 14 shows a set of horizontal slices through the electron density at an altitude of 450 kilometers for various combinations of data sources. It can be seen that the amplitudes of the reconstructions performed using only NNSS or NNSS with GPS are significantly lower than the original image. Using TEC alone, movement is not detected and the reconstruction is extremely sensitive to the satellite location. Adding GPS allows the motion to be detected, however the amplitude of the reconstructions is not accurate. Adding DMSP data causes the reconstruction to be sensitive to satellite location, however the peak heights are much more accurately reconstructed. Using a series of ionosondes as opposed to GPS provides improved peak heights but more difficulty in accurate tracking of the motion. Finally, a combination of GPS and ionosondes to enhance the TEC data appears to provide the best results.

DATA SOURCES	DIMENSIONALITY OF C_s
NNSS	356
NNSS, DMSP	348
NNSS, Ionosonde	300
NNSS, GPS	246
NNSS, GPS, DMSP	238
NNSS, GPS, 3 Ionosondes	219
NNSS, GPS, 7 Ionosondes	200

Table 1. Dimensionality of C_s for various combinations of data sources.

Table 1 shows the dimensionality of C_s as a function of the combination of data sources. Referring to Figure 7, the dimensionality of C_s is the number of degrees of freedom that must be resolved by the smoothness constraints after all of the data is satisfied. Fewer degrees of freedom means that more information was supplied by the data. It is clear from the table that either 7 or 3 ionosondes supply more information than one DMSP satellite and that GPS data from two satellites supply more information than DMSP or ionosonde. The dimensionality of C_s provides a simple way to compare data sources but does not indicate the direction of the dimensions, which can be significant. For instance, the data in Table 1 does not contain the information that GPS data does not supply vertical information.

Suppose the collection of TEC data is modeled as

$$(6)$$
$$Ax = b$$

where the vector x contains the coefficients of the basis functions, the vector b contains the TEC data, and the matrix A converts from image domain to data domain. Then the rank of the matrix A is a measure of the amount of information that is supplied by the TEC data. Figure 15 shows the rank of A in percent of maximum possible rank as a function of number of receivers for static and time varying reconstruction. For static reconstruction the amount of information increases until there are about 9 receivers; more than 10 receivers only provide redundant information. For time varying reconstruction, there is much more information needed for the reconstruction, so the amount if information that can be extracted from the TEC data increases until there are about 23 receivers.

Suppose the collection of additional data consists of only ionosonde data and is modeled by

$$(7)$$
$$Cx = d$$

where the vector x contains the coefficients of the basis functions, the vector d contains the ionosonde data, and the matrix C converts from image domain to data domain. Then the rank of the matrix C is a measure of the amount of information that is supplied by the ionosonde data. Figure 16 shows the rank of C in percent of maximum possible rank as a function of number of receivers for static and time varying reconstruction. The curves for static and time varying reconstruction are almost identical. The amount of information increases approximately linearly until the number of ionosondes approaches the number of pixels in the horizontal direction. However, the curve in Figure 16 does not tell the whole story; the problem with sparse ionosonde coverage is that the resolution tends to be higher directly over an ionosonde than between ionosondes causing distortions in the image.

Conclusions

This paper has presented an initial time-varying algorithm for examining time varying ionospheric features and which removes ionospheric motion as a source for reconstruction degradation. The increased dimensionality of the problem results in a severely underdetermined problem which therefore requires significant additional data sources for accurate reconstructions. The focus of this work has been on the analysis of the effectiveness of various combinations of data sources. Simulations have shown the strengths of GPS for motion detection and the importance of ionosondes for vertical profile estimation.

This initial algorithm was designed for analysis purposes. The major difficulty with any SVD approach is the computation requirements when the problem is scaled up for finer resolution. Considerable future work is needed in order to formulate an algorithm optimized for computation.

Acknowledgements

References

[1] J. R. Austen, S. J. Franke, and C. H. Liu, "Ionospheric imaging using computerized tomography," Radio Science, vol. 23, pp. 299-307, May-June 1988.

[2] G. C. Fehmers, "A new algorithm for ionospheric tomography," Proc. Int'l. Beacon Satellite Symposium, pp. 52-55, July 1994.

[3] P. F. Fougere, "Ionospheric radio tomography using maximum entropy: 1. Theory and simulation studies," Radio Science, vol. 30, pp. 429-444, Mar-Apr 1995.

[4] E. J. Fremouw, J. A. Secan, R. M. Bussey, and B. M. Howe, "A status report on applying discrete inverse theory to ionospheric tomography," Int. J. Imag. Systems Technol., vol. 5, no. 2, pp. 97-105, 1994.

[5] L. Kersley and S. E. Pryse, "Development of experimental ionospheric tomography," Int. J. Imag. Systems Technol., vol. 5, no. 2, pp. 141-147, 1994.

[6] G. R. Kronschnabl, G. S. Bust, J. A. Cook, and C. J. Vasicek, "Mid-America computerized ionospheric tomography experiment (MACE '95)," Radio Science, vol. 30, pp. 105-108, Jan.-Feb. 1995.

[7] H. Na and C. Biswas, "Localized space-frequency algorithm for computerized ionospheric tomography," Radio Science, vol. 31, no. 6, pp. 1555-1566, 1996.

[8] T. D. Raymund, "Comparisons of several ionospheric tomography algorithms," Annales Geophysicae, vol. 13, pp. 1254-1262, Dec. 1995.

[9] E. Sutton and H. Na, "Ionospheric tomography using the residual correction method," Radio Science, vol. 31, pp. 489-496, May -June 1996.

[10] E. Sutton and H. Na, "Static tomographic reconstruction of the time varying ionosphere," Proc. ICIP-96, Vol. III, (Lausanne, Switzerland), pp. 523-526, IEEE Signal Processing Society Press, Sept. 1996.
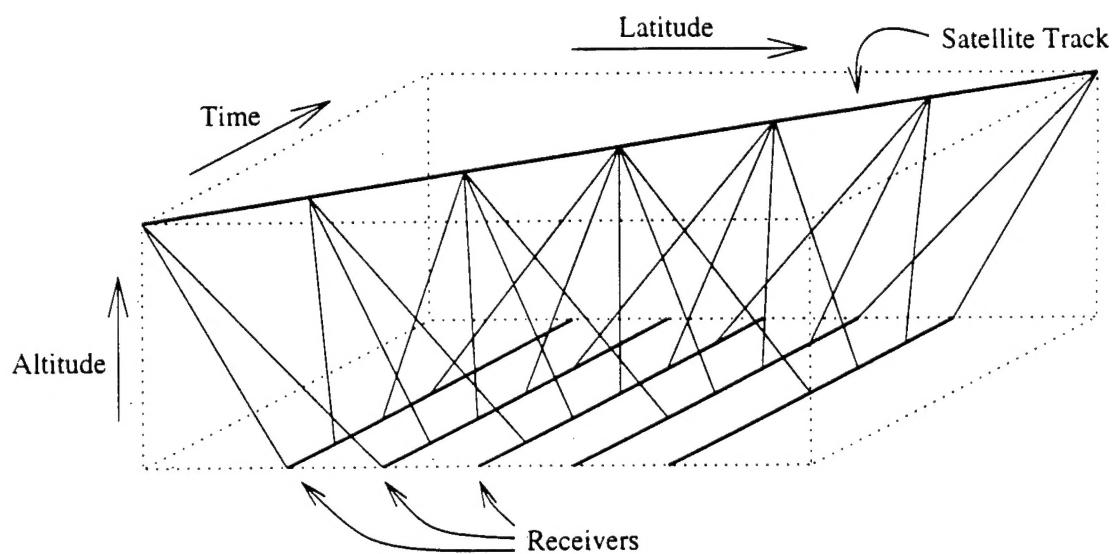
Figure 1. Three-dimensional system model of TEC data acquisition.
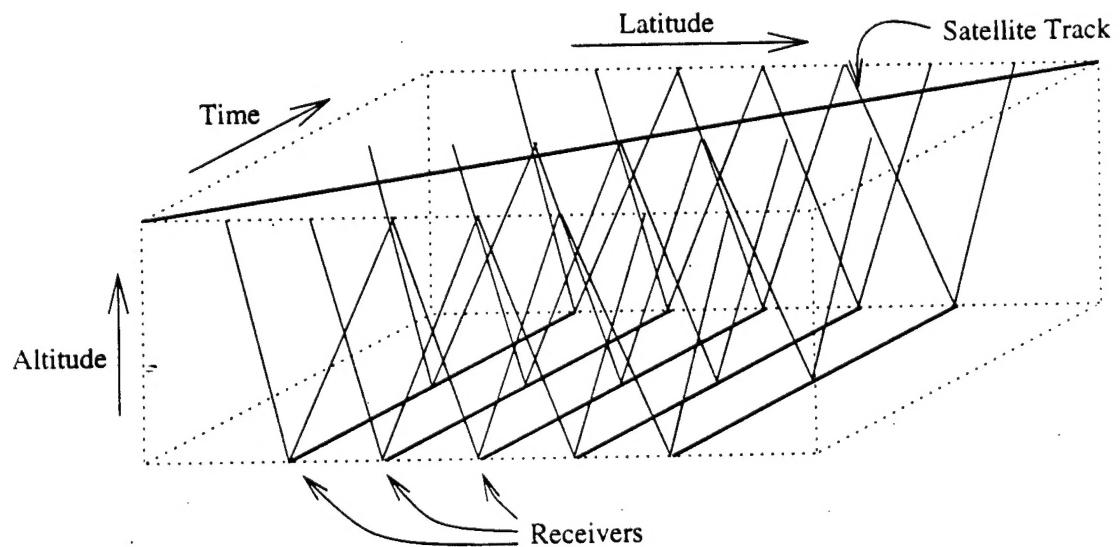
Figure 2. Three-dimensional system model of GPS data acquisition.

Latitude →   Satellite Track

Time ↗

Altitude

Receivers
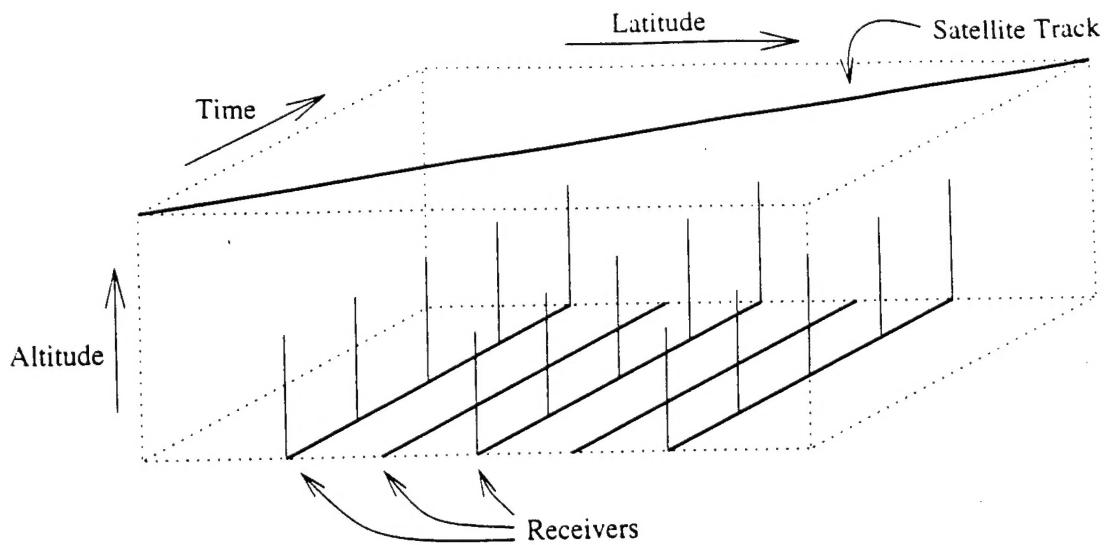
Figure 3. Three-dimensional system model of ionosonde data acquisition.

Latitude →   Satellite Track

Time ↗

Altitude

Receivers
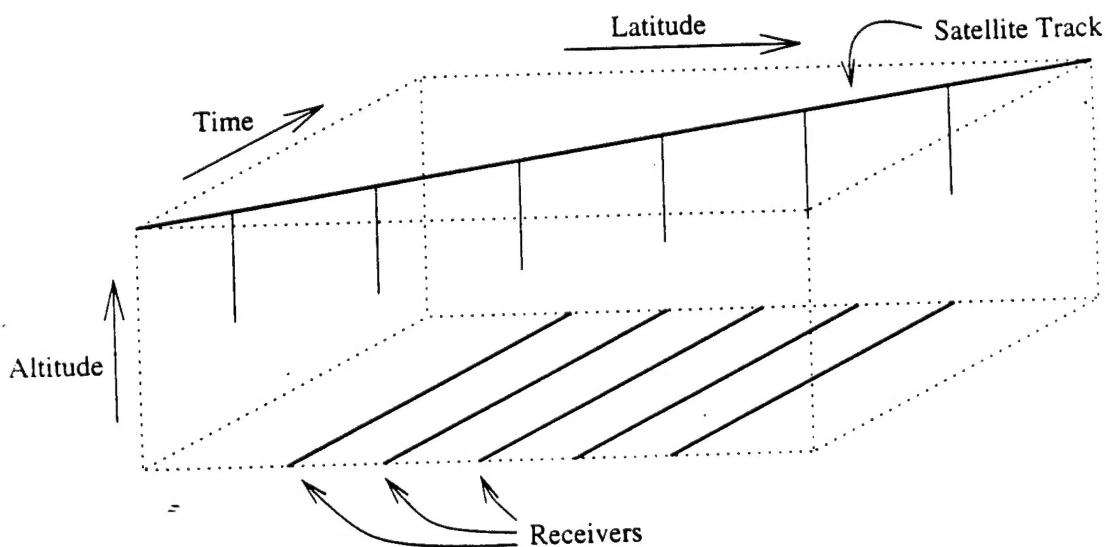
Figure 4. Three-dimensional system model of DMSP data acquisition.
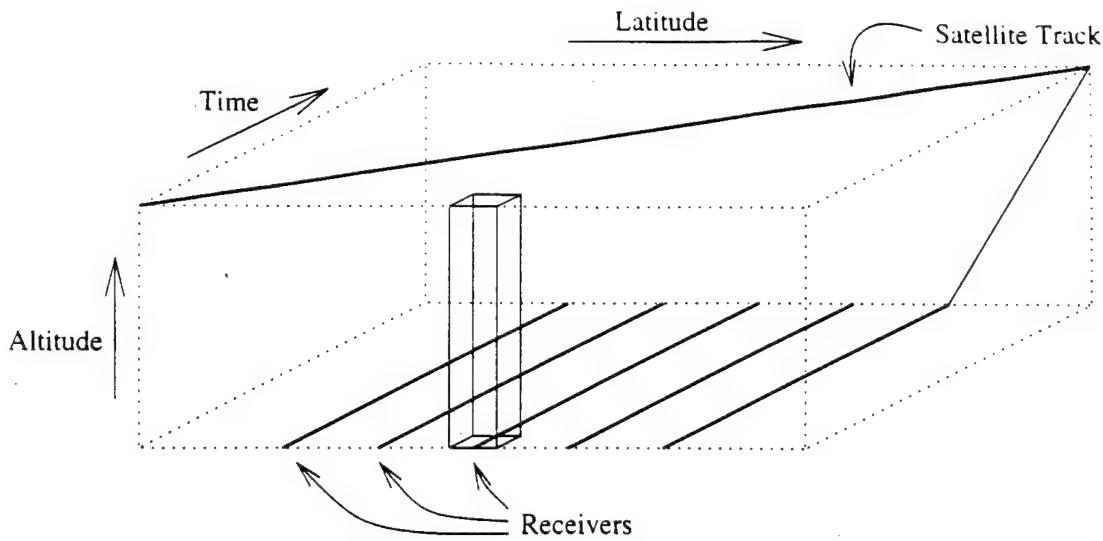
Figure 5. Three-dimensional basis function used in TVCIT algorithm.
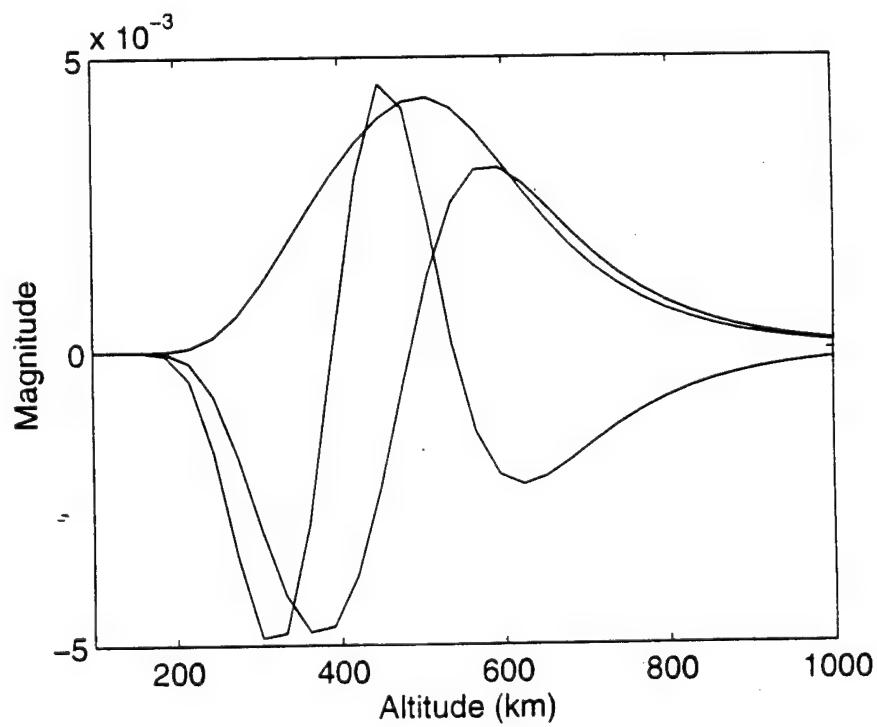
Figure 6. Example of three vertical basis functions used in TVCIT algorithm.
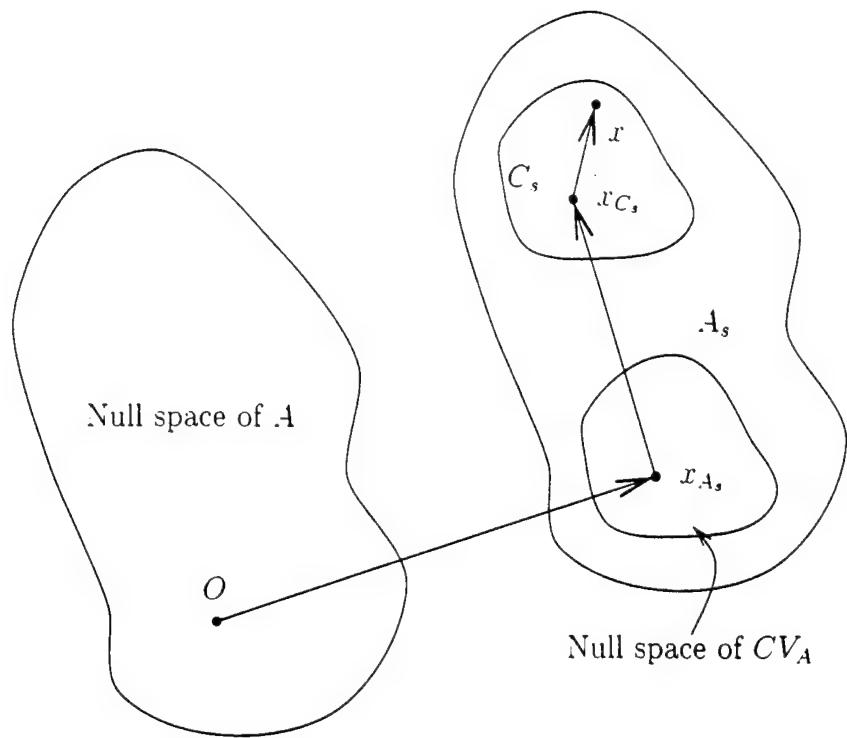
Figure 7. Diagram of reconstruction process used to resolve multiple sources of data.
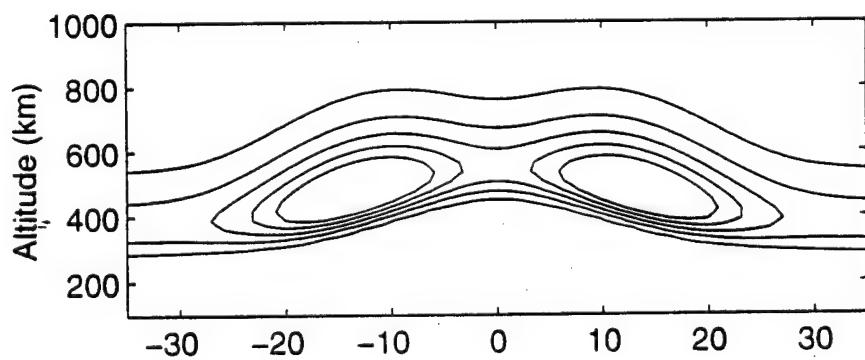
Figure 8. Original image used in reconstructions. Contours graphed at normalized densities, from outer extremes to the center peaks, at 0.4, 0.6, 0.8, 1.0, 1.2.
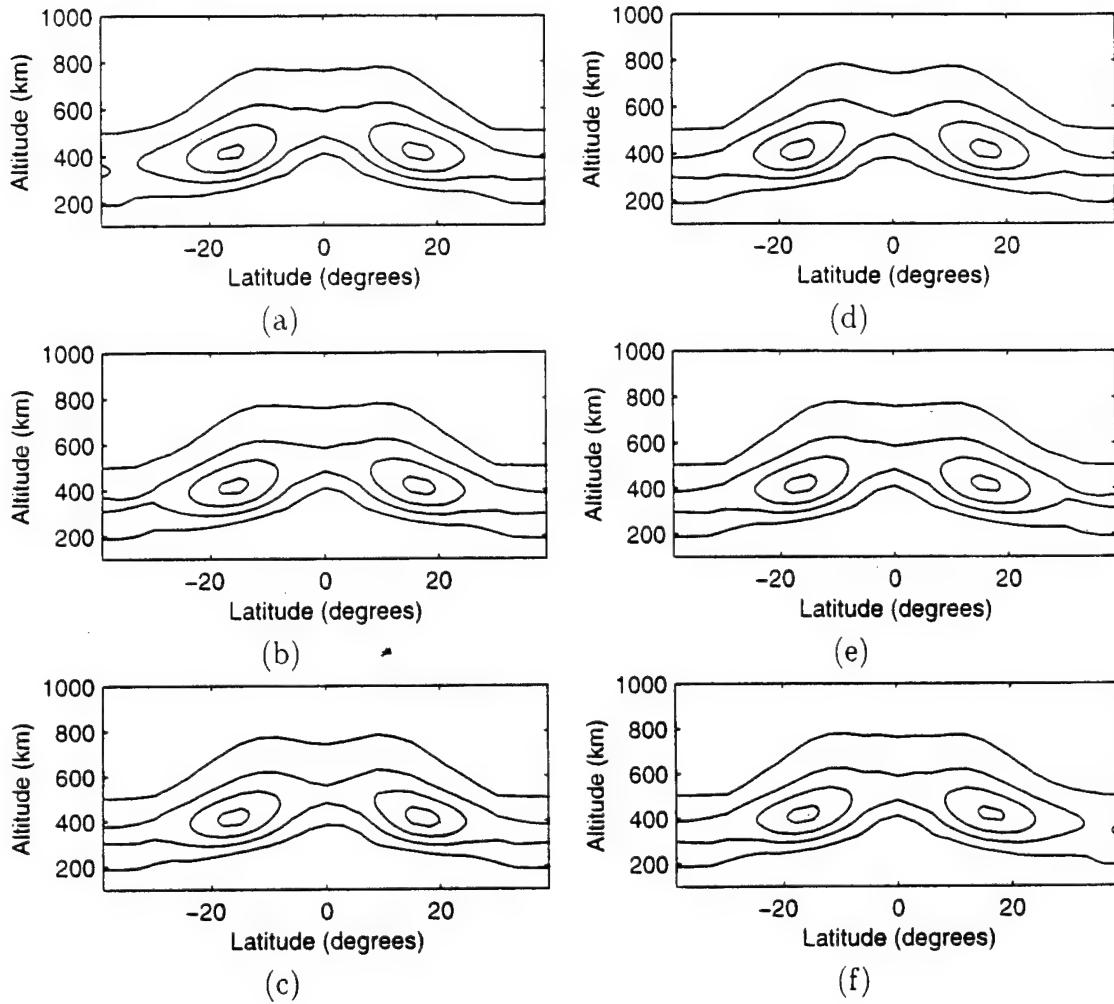
Figure 9. 6 time slices of a reconstruction of a static ionosphere using the TVCIT algorithm. A combination of NNSS, GPS and ionosonde information is used. Contours graphed at normalized densities, from outer extremes to the center peaks, at 0.2, 0.6, 1.0, 1.4.
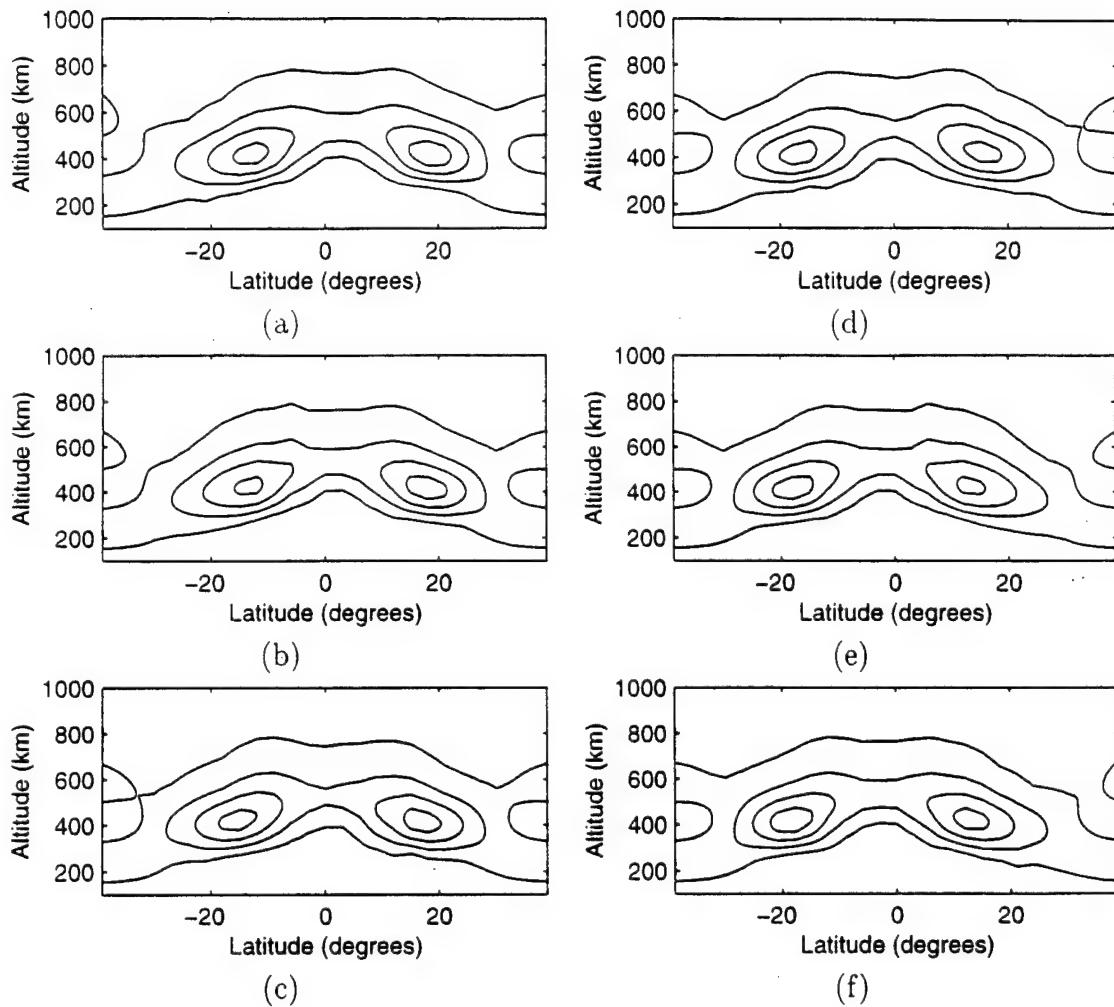
Figure 10. 6 time slices of a reconstruction of an ionosphere moving north (right) by 5
degrees, using the TVCIT algorithm. A combination of NNSS, GPS and
ionosonde information is used. Contours are graphed at normalized densities,
from outer extremes to the center peaks, at 0.2, 0.6, 1.0, 1.4.
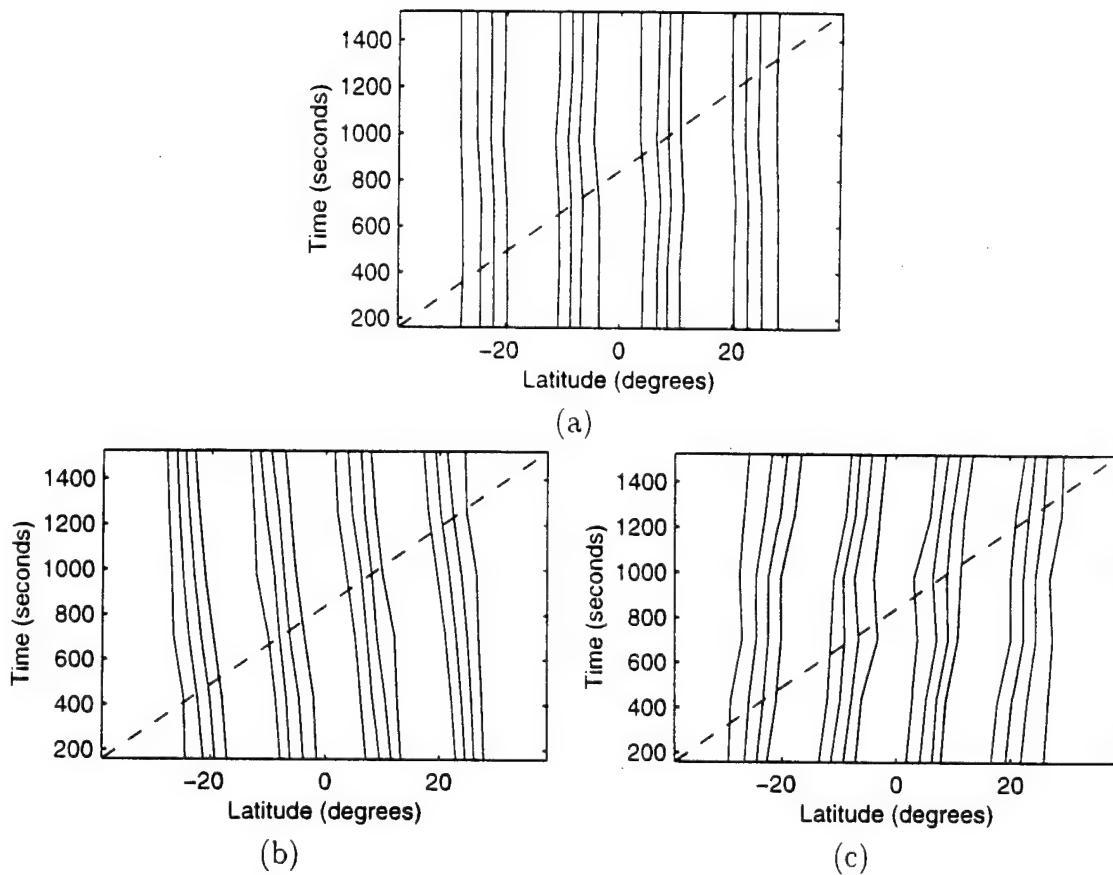
Figure 11. Horizontal slices through the 3-dimensional reconstructed volume, formed
using NNSS, GPS, and ionosonde data, at a fixed altitude of 450km.
(a) Horizontal slice through a reconstruction of a static ionosphere.
(b) Horizontal slice through a reconstruction of an ionosphere moving south
(left) by 5 degrees. (c) Horizontal slice through a reconstruction of an ionosphere
moving north (right) by 5 degrees.
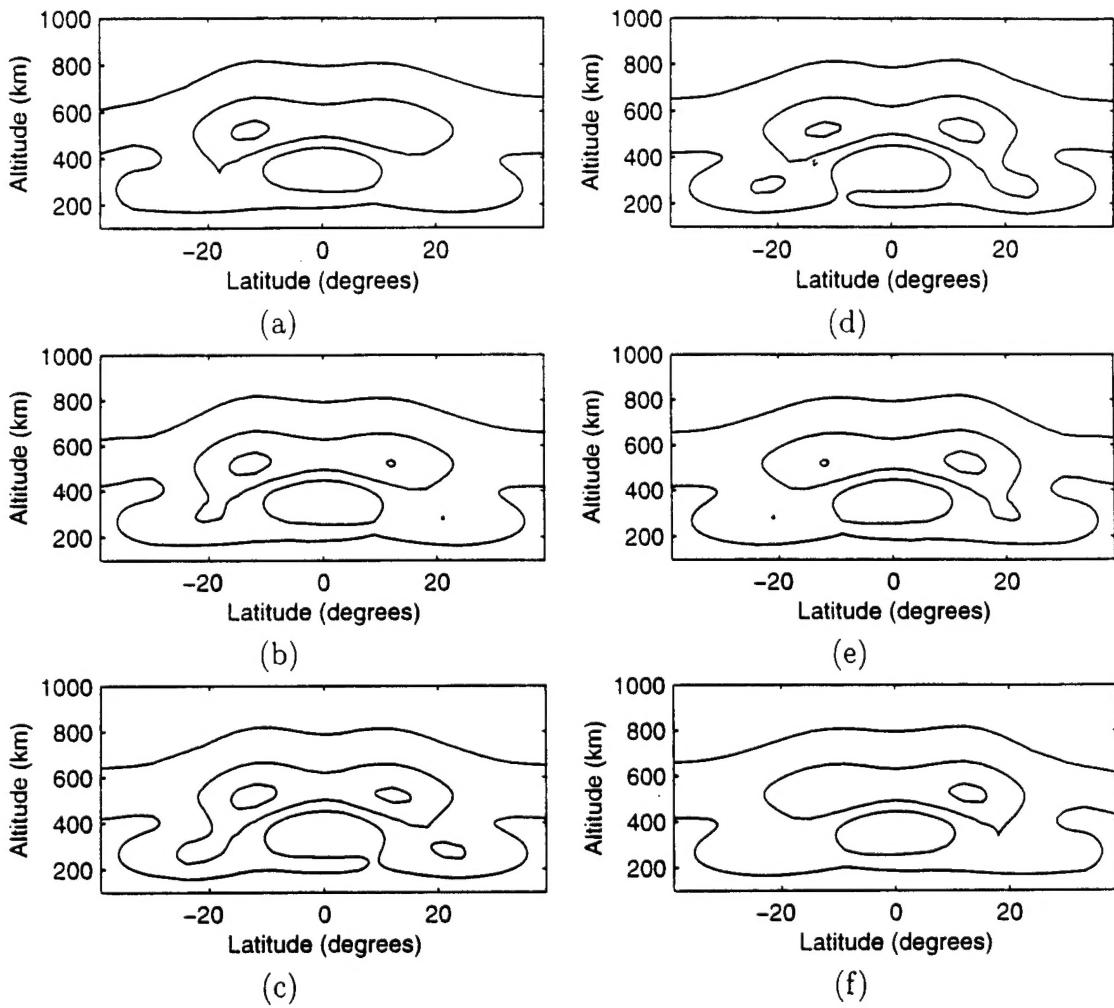
Figure 12. 6 time slices of a reconstruction of an ionosphere moving north (right) by 5 degrees, using the TVCIT algorithm using only NNSS TEC data. Contours are graphed at normalized densities, from outer extremes to the center peaks, at 0.2, 0.6, 1.0, 1.4.
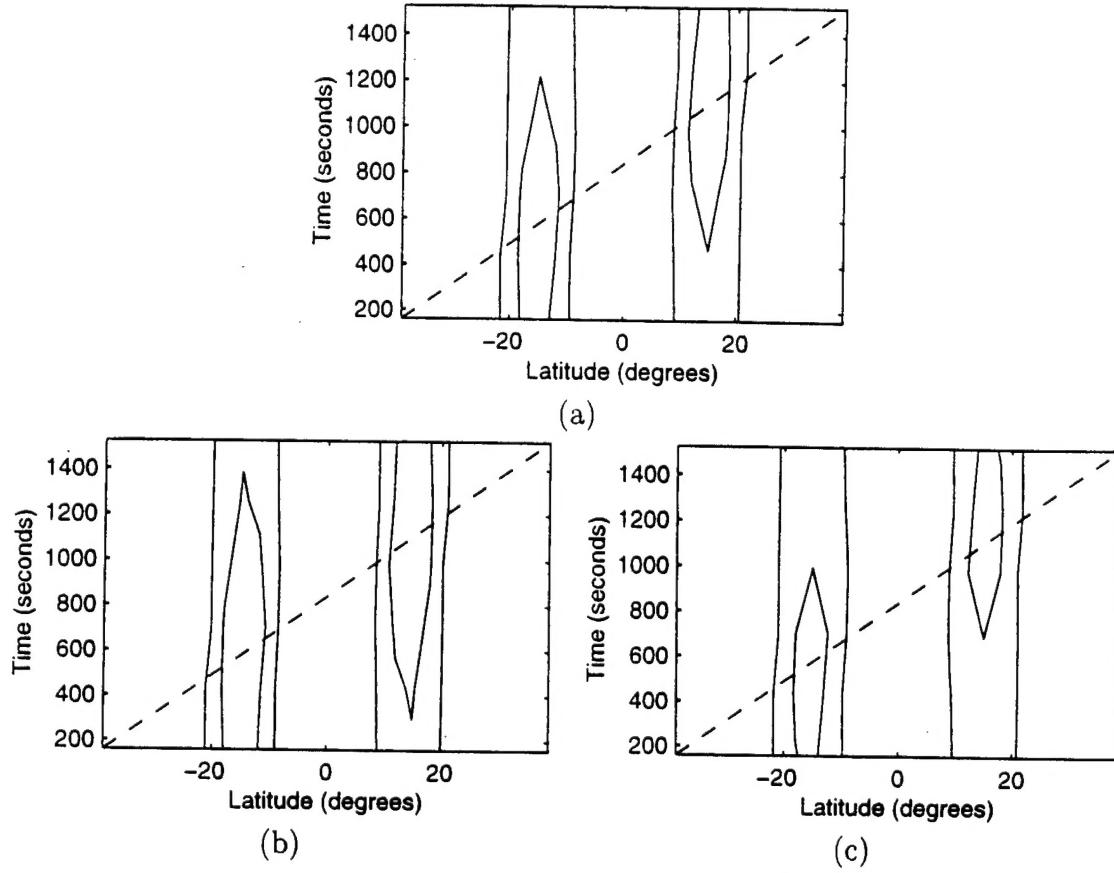
Figure 13. Horizontal slices through the 3-dimensional reconstructed volume, formed from NNSS TEC data only, at a fixed altitude of 450km. (a) Horizontal slice through a reconstruction of a static ionosphere. (b) Horizontal slice through a reconstruction of an ionosphere moving south (left) by 5 degrees. (c) Horizontal slice through a reconstruction of an ionosphere moving north (right) by 5 degrees.
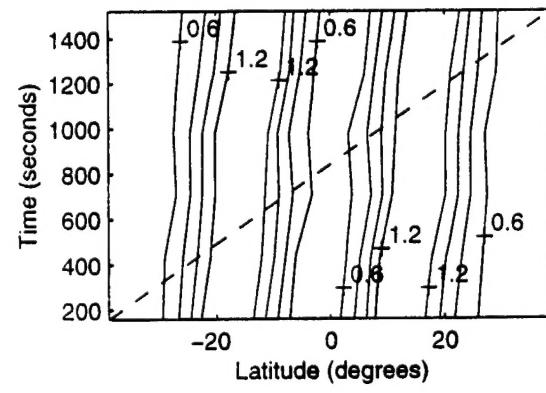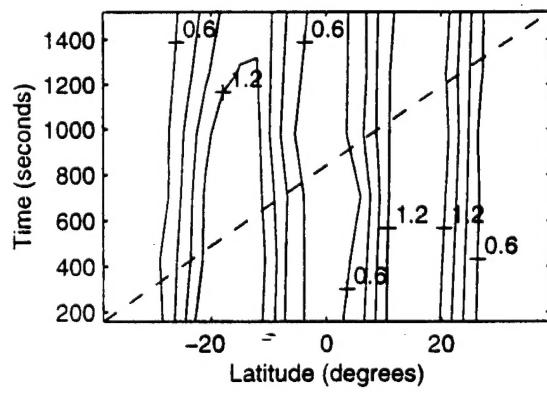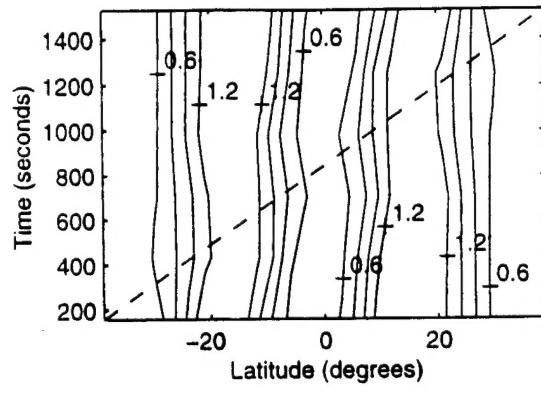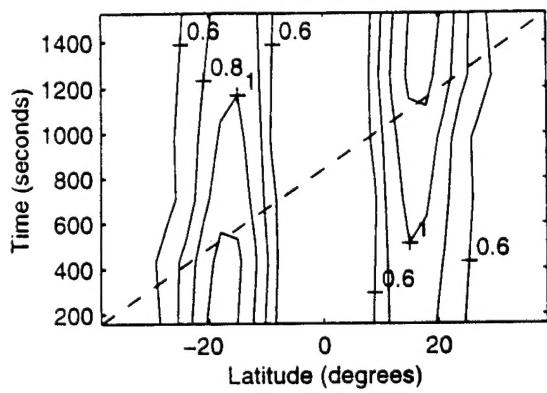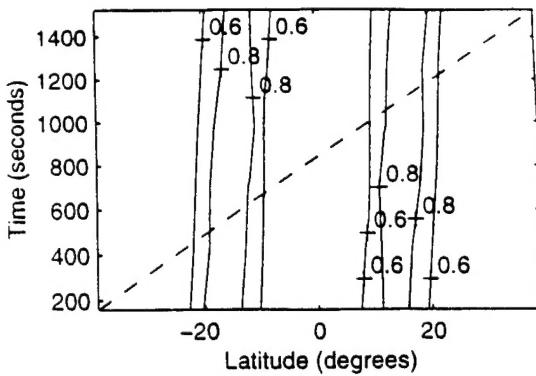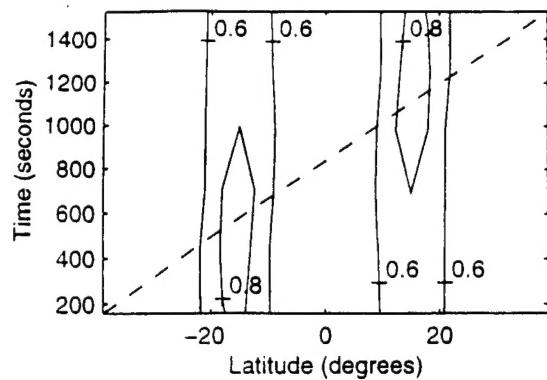
Figure 14. Horizontal slices through 3-dimensional reconstructions at 450 km, using
(a) NNSS data only (b) NNSS and GPS data (c) NNSS, GPS and DMSP data
(d) NNSS and ionosonde data (e) data from NNSS, GPS and 3 ionosondes
(b) data from NNSS, GPS and 7 ionosondes.
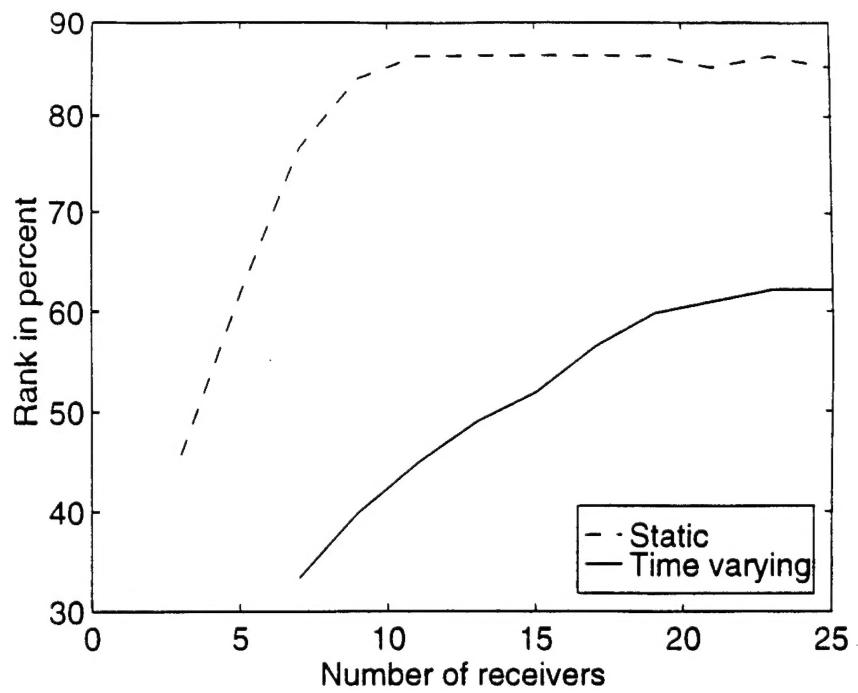
Figure 15. Comparison of the information contained in TEC data as a function of the number of receivers, for both static and time varying reconstruction.
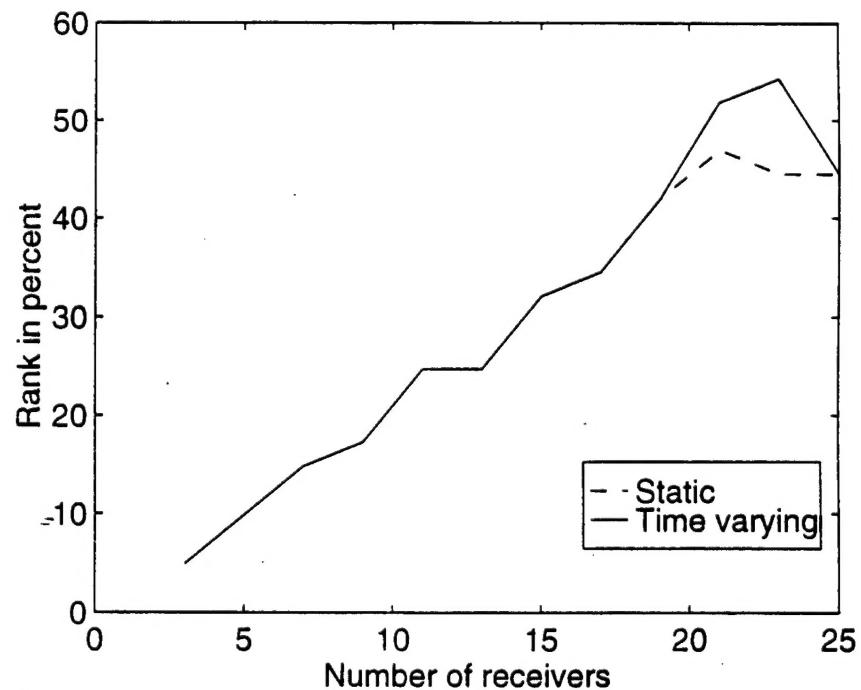

Figure 16. Comparison of the information contained in ionosonde data as a function of the number of receivers, for both static and time varying reconstruction.